International Journal of Engineering Research & Technology (IJERT)
ISSN: 2278-0181
Vol. 4 Issue 02, February-2015

The Method of Using slices to Estimate the Noise Power Spectrum of A Medical X-Ray Imaging System

Zeki Ahmed Darwish [1]
Sharjah Education Zone
Ministry of Education
United Arab Emirates
PO.Box 10784

Wan Muhamad Saridan Wan Hassan [2]
Department of Physics
Faculty of Science
UniversitiTeknologi Malaysia
81310 UTM Skudai, Johor DT, Malaysia

Amer Al Nassiri [2]
College of Information technology
University of Ajman of Sciences & Technology
PO. Box 4636 Fujairah, United Arab Emirates

Hussain Al Alawadhi [2]
Department of Physics
Faculty of Science
University of Sharjah,PO.Box 27272
United Arab Emirates

***Abstract*—This paper presents Dobbin's method to estimate the noise power spectrum using a screen film system. The one-dimensional spectral estimate was obtained by extracting thick and thin slices from two-dimensional noise power. The slices were made parallel to the primary axis of ROI, but did not include the axis. We measured NPS using one slice, two slices, four slices, eight slices,upper eight slices (a) and eight slices (b) of data in the 128×128 two-dimensional NPS space which were extracted to generate the one-dimensional NPS curves in horizontal and vertical directions and they were compared with Dobbin's method. Very little was found in the NPS shape with regards to the two-dimensional space only and the slice which contained one row and one column was sufficient to study NPS in the two-dimensional space**

Keywords—X-ray, Noise power spectrum, screen film system, fast Fourier transform

I. INTRODUCTION

The noise power spectrum (NPS) is an important concept that has been widely accepted for quantitative evaluation of image quality both in clinical practice and in research. The radiographic noise may be calculated from the Fourier transform either of the autocorrelation function (the indirect method) or from the square of the modulus of the Fourier transform of the data itself (the direct method) [1]. Screen film system has been used in conventional radiography examinations by capturing the pattern of x-rays transmitted through a patient. Recently, however, as problems with screen film based medical imaging systems have become clearer, improvements in digital radiography (DR) technology have been researched to resolve such problems [2]. There are several digital radiography systems, which include computed radiography (CR), flat panel detector, and charge coupled device (CCD) based systems [3]. The Wiener spectrum (WS) represents the noise power spectrum in an image as a function of spatial frequency. It, therefore, represents the relationship between noise and spatial resolution [4, 5, and 6]. Wiener spectrum (WS) provides the means of characterizing image noise and plays a central role in the ultimate measuring of image quality. The noise in images is recognized as an important factor in determining image quality. Image noise may be characterized by the WS or the noise power spectrum (NPS) [7]. To evaluate the detector's performance, one must calculate the quantitative values of image acquired by digital x-ray detectors such as a noise power spectrum (NPS), modulation transfer function (MTF), noise equivalent quanta (NEQ), and detective quantum efficiency (DQE) [8]. This study focuses on the noise power spectrum using only Dobbin's method.

As far as the indirect method (slit synthesis method) is concerned, noise properties were studied in the spatial domain by Doi (1966) [9], Wagner (1977) [10], Sandrik and Wagner (1981) [11], Doi (1986) [12], Koedooder (1986) [13], Cowen and Workman (1990) [14] and were developed by Wan (2001) [15]. The current study deals with NPS in frequency domain, a direct method which was used to compute the total 2-D NPS. Two main reasons for computing the entire 2-D NPS are important. First, numerous artifacts in 2-D NPS were found that would not have been found if a one-dimensional version had been computed using the slit synthesis method. Second, only a finite amount of image noise data was available for use in order to produce the best estimate of true NPS (Dobbins III, 1995) [4]. NPS computation has been based on the work of Dobbins, Williams (1999) [16], Suryanarayanan (2004) [17], Park (2008) [18], Lazzari, (2007) [19] and Zhang (2008) [20]. On terms of comparison between the method of Wagner (indirect method) and Dobbins to measure the NPS of medical imaging system, the two methods agree on the practical value of noise power spectrum between10^{-3}-10^{-6} mm^{-2} over the spatial frequency range 0-10 mm^{-1}.It was found that Dobbins's method was easier to implement for studying the

NPS [21]. The NPS measurements were compared as one slice, two slices, four slices, eight slices upper, eight slices (a) and eight slices (b) of data in the 128×128 two-dimensional NPS space which were extracted to generate the one-dimensional NPS curves in the horizontal and vertical directions. There was very little difference in the NPS shape with regard to the two dimensional space only. We found that the slice contains one row and that one column was sufficient to study NPS in the two-dimensionalspace.

II. DOBBIN'SMETHOD

A Kodak Lanex Regular TMG screen-film system (SF) was used for measurement. Image A3.bmp was prepared by exposing the Kodak Lanex Regular TMG screen –film with 80 kV_PX-ray, with a 16 mm thick aluminum filter affixed to the X-ray tube window. The focus-to- film distance was 1.5 m. The analog image is a spatially varying signal in a plane. It can be expressed as a function of a continuous variable such as (x, y), representing a two-dimensional position in the image. Optical density distribution in a radiographic film is an analog image. In this work, the image A3.bmp is a digitized image obtained from analog images by scanning. The uniform background area of the film was scanned using a microdensitometer. This scanning gave the image A3.bmp. The size of the scan was 1000×1000 pixels corresponding to a physical area of 1.25 cm by 1.25 cm and 978-590 pixels corresponding to a physical area of 1.22 cm by 0.74 cm (see Table 1).

Table 1: Detailed information on the image used in this research.

Name	Image System	Image Size (cm)	Digital Matrix	Pixel Size
A3.bmp	SF	1.25×1.25	1000×1000	12.5µm

After the image is read, the pixel value is converted to optical density before the data is processed by the NPS routine. A 978×590 pixel region of interest ROI was cropped and used in computing the average image. Calculation of number of segments available was done in order to calculate the mean density of ROI_S using the following equation:

Difference image(x, y) =image(x, y)-average image(x, y) (1)

Non-overlapping 128×128 ROI_S were chosen from one image to obtain many ROI_S for each acquisition combination. These ROI_S were used in computing the ensemble average of squares of magnitude of Fourier transformed images, and the raw NPS was estimated as described by Dobbins III. (1995).

$$NPS(u,v) = \frac{\left\langle |FFT(difference\ image(x,y)|^2 \right\rangle}{N_x N_y} \quad (2)$$

where$\Delta x$and Δy are the pixel pitch in$x$ and$y$directions, respectively, (Δx= 12.5 µm, Δy=12.5µm),$N_x$and N_y are the number of elements in the$x$ and y direction respectively,N_x=N_y=L=128.Then, the normalized NPS (NNPS) was obtained using thefollowing equation

$$NNPS = \frac{NPS(u,v)}{L^2} \quad (3)$$

One-dimensional NPS in horizontal and vertical direction was obtained by averaging 4 slices on either side of the horizontal axis and 4 slices on either side of the vertical axis of the 2-D NPS as in Fig.1.

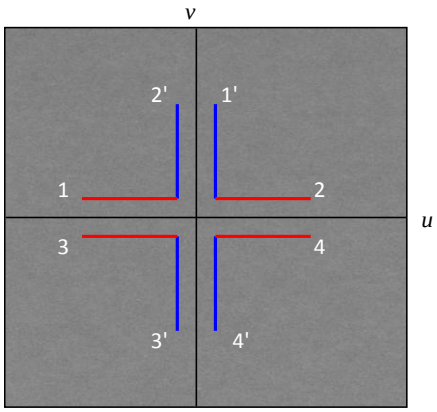

Fig.1 Slices used to generates horizontal and vertical 1-D NPS.

II. METHODOLOGY

Notably, in the context of the evaluation of slice method, 1-D spectral estimate has been obtained by extracting thick and thin cuts from the 2-D noise power spectrum. The cuts are made parallel to the primary axis, but do not include the axis, in order to avoid low-frequency trending effects. To evaluate this approach for analysis of the noise power spectrum, we use in this study one cut along the primary v axis and one cut along the u axis.

A. One slice adjacent to axis

Fig.2 illustrates the row 1 and column 1' slices which are adjacent to u and v-axis respectively in order to measure the one-dimension NPS in horizontal and vertical directions. The NPS values were measured using image A3.bmp, pixel size 0.0125 mm, Fourier length 128 with non-overlapping 28 sub_ROI of 978×590.

The 2D-NPS curve is obtained by taking the average of horizontal and vertical 1D-NPS with spatial frequency defined as

$$w = \sqrt{u^2 + v^2} \quad (4)$$

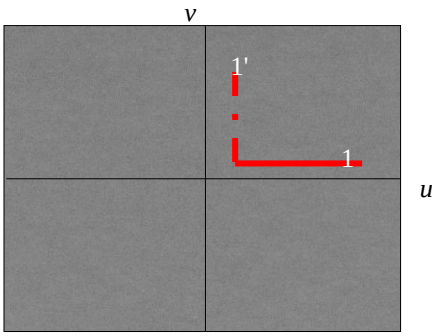

Fig.2Slices used to generate horizontal and vertical 1-D NPS.

B. Two slices adjacent to axis

We choose two rows of NPS data (1, 2) above *u* axis on the left and the right axis and two columns (1', 2') just adjacent *v* axis as in Fig.3. These rows and columns NPS data are used to generate 1-D and 2-D NPS curves.

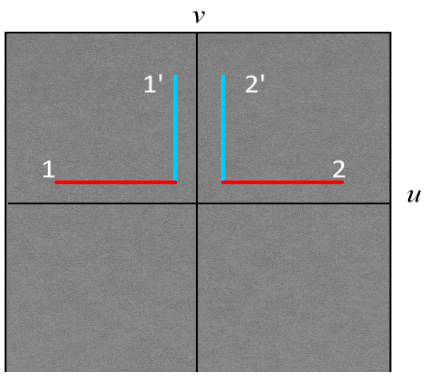

Fig.3 Two rows (1, 2) and columns (1', 2') were used to generate horizontal and vertical 1-D NPS.

C. Eight Slices upper u-axis

Four rows (1, 2, 3, 4) and four columns (1', 2', 3', 4') of data just above the u axis were in the 32×32 two-dimensional NPS space and were extracted to generate 1-D NPS curves in horizontal and vertical directions by averaging the NPS values of the 4 rows and 4 columns as in Fig.4. A 2-D NPS is defined by averaging the horizontal and vertical 1-D NPS.

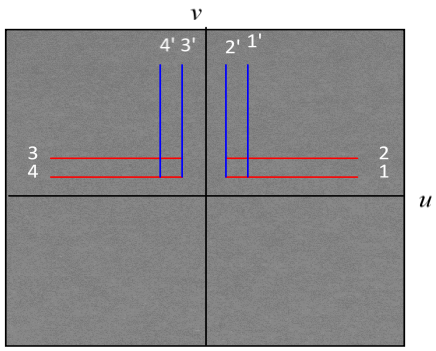

Fig.4 Rows and columns, data used to generate horizontal and vertical 1-D NPS.

D. Eight adjacent lines

Figs. 5 (a) and (b) show the eight rows (1, 2, 3, 4, 5, 6, 7, 8) and columns (1', 2', 3', 4', 5', 6', 7', 8') of data in two cases of 128×128 two dimensional NPS spaces that were extracted to generate the 1-D NPS curves in the horizontal and vertical directions.

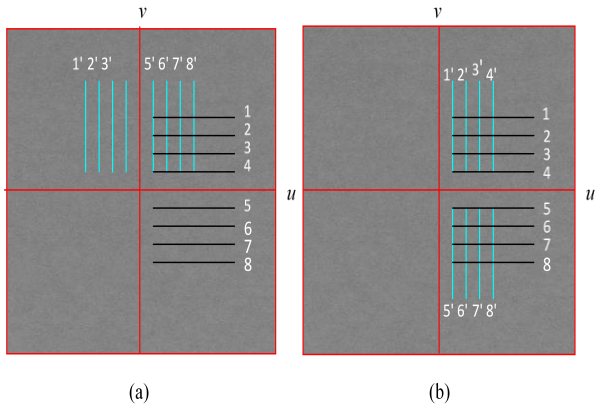

Fig.5 Eight slices used to generate vertical and horizontal 1-D NPS in two different cases.

IV. RESULTS AND DISCUSSION

A. Comparison of NPS Esitmates from Different Slices

One line, two lines, four lines, eight lines upper, eight lines (a) and eight lines (b) in Figs (1,2,3,4, and 5) of data in the 128×128 two-dimensional NPS space was extracted to generate the one-dimensional NPS curves in the horizontal and vertical directions sections. There was very little difference in the NPS shape with regard to the two-dimensional space as shown in Fig.6.

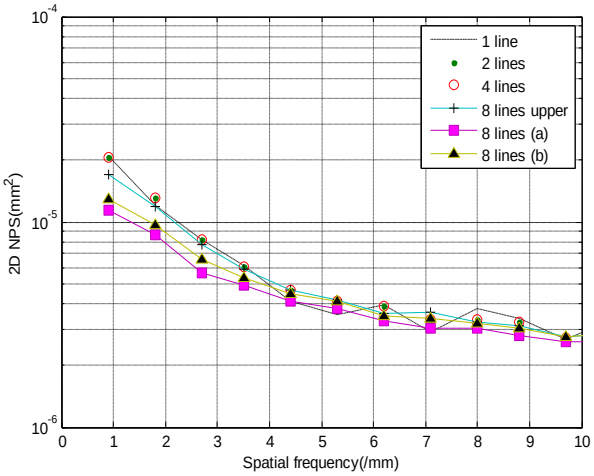

Fig. 6 2D- NPS values for the different slices.

Fig.7 shows the one-dimensional NPS_s in the horizontal direction. We found that the NPS curves dropped gradually until to the frequency 10 mm^{-1} in addition the NPS curves for one, two lines, four lines were identical in horizontal direction, but different in the vertical direction as shown in Fig.8.

B. Normalized Noise Power Spectrum

The NPS is most commonly computed directly from the squared Fourier amplitude of two-dimensional image data using Equation 2. Conventionally, the Fourier transform is normalized by dividingN_x,N_y. Here$N_x$andN_y are the number of pixels in$x$ and $y$directions. Often, the noise power spectrum is normalized further by dividing it with a large area signal squared as follows:

$$NNPS = \frac{NPS(u,v)}{(\text{large area signal})^2} \quad (5)$$

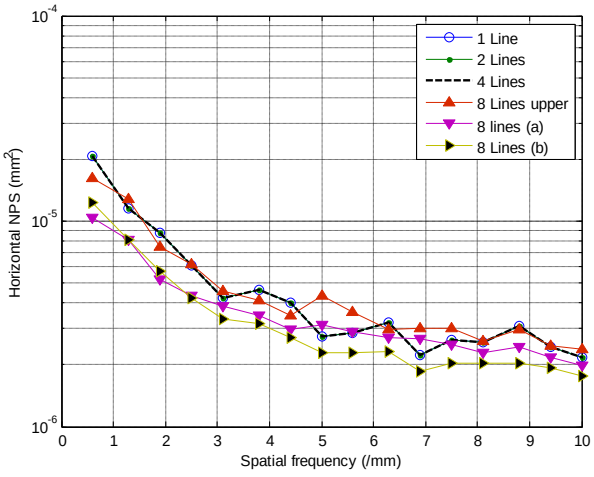

Fig.7 1-D NPS (horizontal) values for the different slices.

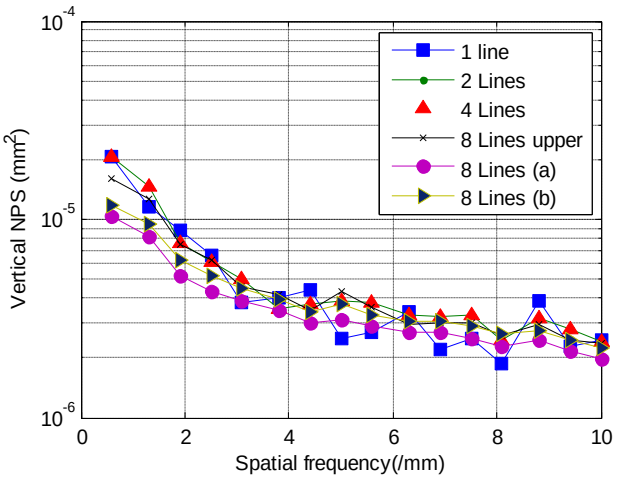

Fig. 8 1-D NPS (vertical) values for different slices.

The large area signal is a measure of the gain of the system (i.e. what value is recorded for a particular exposure incident on to the system). It is measured in the same units as the data used to determine NPS. The signal level may vary from one ROI or image to another, NPS was normalized to the mean image squared (Large area signal) ^{2} or (L^2), computed for the ROI was used to eliminate the direct effect of signal variation, with the result, NPS/L^2, referred to as the normalized NPS [22]. This normalization was done by averaging 28 non-overlapping segments of image A3.bmp. The two-dimensional normalized NPS was converted into a one- dimensional normalized NPS along horizontal and vertical directions by averaging the two-dimensional data over four lines above and four lines below the horizontal axis and four lines to the right of and four lines to the left of the vertical axis, respectively. Fig.9 shows the normalized NPS curves.

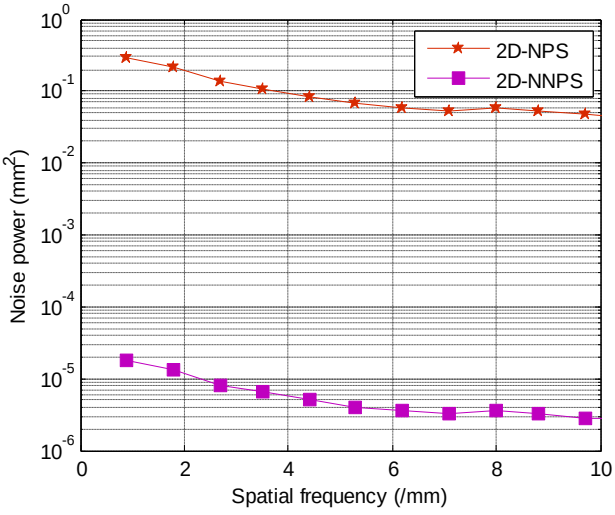

Fig. 9. Normalized 2-D NPS taken from 4 slices adjacent to the *u* and *v*-axis.

C. Overlapping and Non-overlapping ROI

Fig. 10 shows the overlapping blocks with an overlap of 4 points in the*x* direction. Each 4-by-8 block has 4 columns which overlap in the*x* direction.

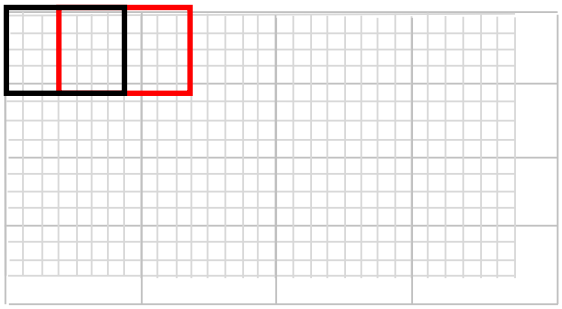

Fig.10. Image divided into distinct blocks with specified overlaps.

The overlapping and non-overlapping subgroup of a 978 ×590 image matrix of A3.bmp were 64×64, 128×128, and 256× 256, respectively. Asfar as the radial two-dimensional NPS of the 64×64 ROI with overlap and no overlapis concerned, there was a small difference in the NPS estimate. For the 128×128 ROI, it was found that no difference existed in the NPS curves. In this particular case, the larger ROI size demonstrated the worse results of measurements as in Fig.11. It was found that more fluctuations existed in the NPS curve when the ROI size was large.

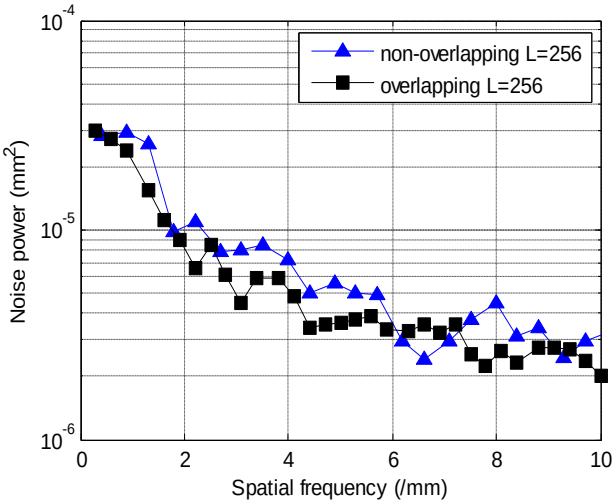

Fig.11NPS values for the 256×256size of overlapping and non-overlapping ROI.

D. Size of Region of Interest ROI

An increase in the size of the ROI will tend to reduce the number of segments as well as change the area under the horizontal and vertical NPS curves. The volume under the 2-D NPS does not change. For example, Fig.12 shows the choice of ROI from image A3.bmp. Fig.13 shows the effect of the smaller ROI size (32×32 pixels) in the calculation upon the NPS. Generally, when ROI is small, the curves are smoother in the one and radial two-dimensional directions. When plotting the total two- dimensional NPS in the surface plot (3-D), the highest peak is clear in Fig.14 and become sharper when the ROI size isincreased

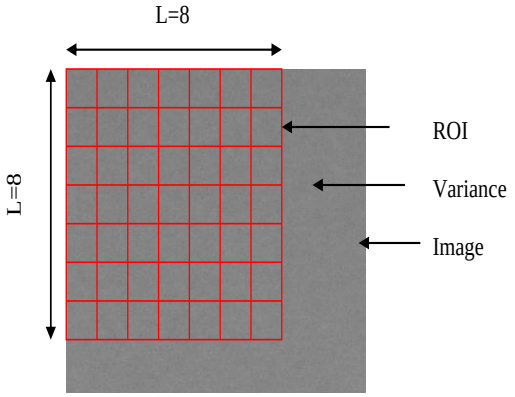

Fig.12. Choice of ROI from original Image A3.bmp.

Fig.15 illustrates thefactthat, the bigger the ROI size (256×256), the greater the fluctuations which exist in the NPS curves in radial two-dimensional and one-dimensional and vertical directions.Fig.16 shows the final overall comparison of ROI_S 32×32, 64×64, 128×128, 256×256 sizes, in which it was found that the NPS curve was higher compared to other curves.

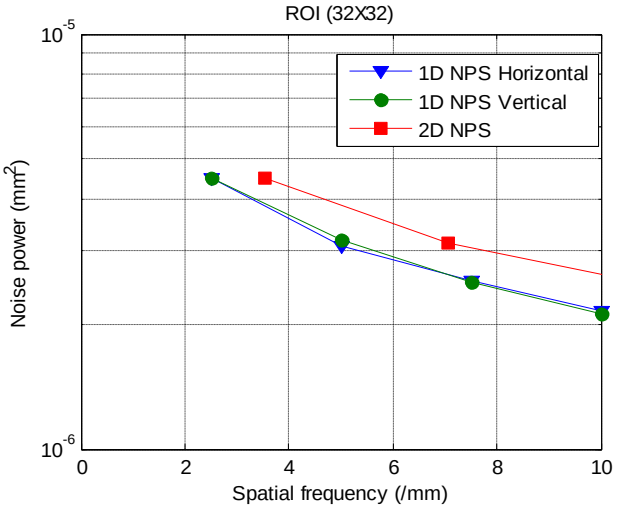

Fig.13 1-D NPS horizontal, vertical and 2-D NPS values for 32×32 ROI.

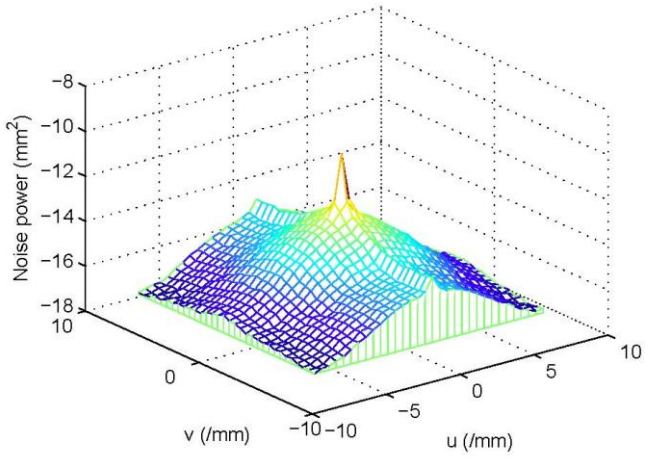

Fig. 14 Meshz plot of 2-D NPS for 32×32 ROI.

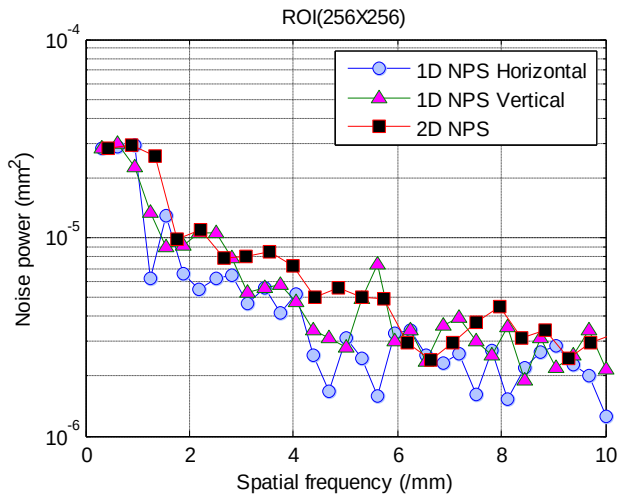

Fig.151-D NPS horizontal, vertical and 2-D NPS values for 256×256 ROI.

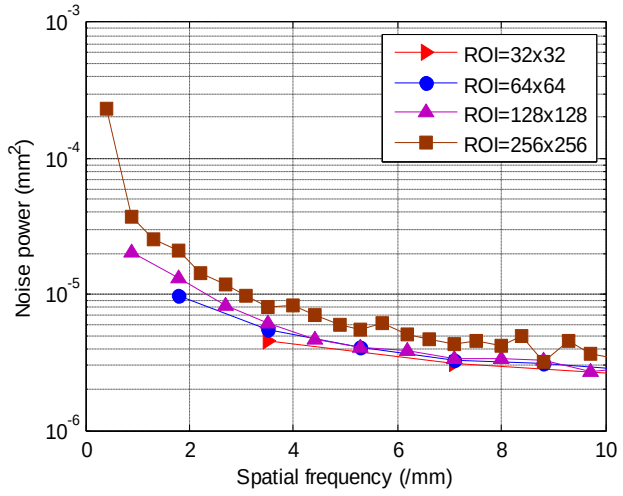

Fig.16 Comparison of the NPS values for various ROI sizes.

E. Aradial symmetric NNPS

A radial symmetric 2-D NNPS of the ROI in rectangular coordinates was calculated and the total 2-D NPS was determined as it is a square module. The final 2-D as the ensemble average was derived for every frequency (*u*, *v*) as an arithmetic. The average of all available ROIs was calculated. 1-D NPSs can be obtained using the different methods which we suggested in section III and other methods used by Dobbins [4], [23] and [24]. In this case, we used 4 lines as in section II to calculate 1D-NPS(Vertical and Horizontal directions) and2D- NPS (*u*, *v*). The frequency value (w_{ij}) was computed from Equation 4 and the interval sampling frequency (0.6250mm^{-1}).

As a numerical example, the functions of spatial frequency variable u are now evaluated at discrete frequencies given by$u=k\Delta u,k=0, \pm1, \pm2, \pm3$ ….The maximum spatial frequency sampled, the Nyquist frequency, is$u_n=1/(2dx)$ =40mm^{-1}, where$dx=0.0125mm$, Fig.17 shows a set of radial symmetric NPS curves. A radial two-dimensional NPS represents a part of the total noise power spectrum in an image. The total 2-D NPS is represented in the imaging systems by mesh plot (surface), with Fig.14 showing the total noise power spectrum in image A3.bmp.

III. CONCLUSION

By Dobbins's method, the entire 2-D NPS was calculated from the square modulus of the Fourier transform of the data itself (the direct method) according to equation 2. The one- dimensional NPS was obtained by extracting slices from 2-D noise power spectrum, with the slice made parallel to the primary axes. One line, two lines, four lines, eight lines of data in the 128x128 two dimensional NPSspaces were extracted to generate the one-dimensional NPS curves in the horizontal and vertical directions. It was found that there is no

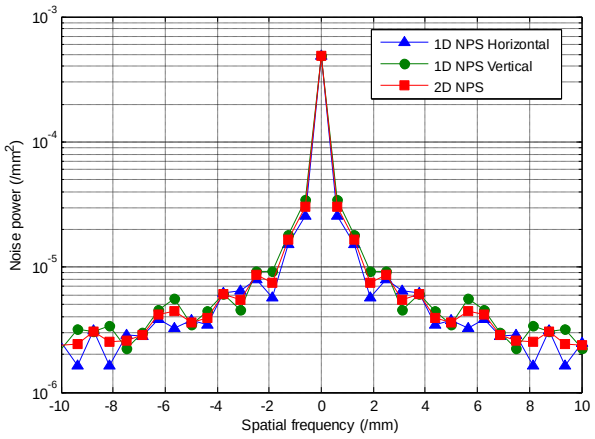

Fig.17 A setof radial symmetric NPS values, 2-D and 1-D horizontal and verticalvalues.

difference in the radial two-dimensional NPS shapes for different lines. The normalized NPS (NNPS) was obtained using Equation4 in keeping with the work of Dobbins III (1995). The overlapping and overlapping ROI_s for 64×64, 128×128 and 256×256 were at pixel value 0.0125 mm, whereas, for the smallest ROI, there was a small difference in the NPS curves. For the 128×128 ROI size, there was no difference in NPS curves while in the bigger ROI it was found that the NPS curves had more fluctuations. In the last section, we explained the difference between the radial two-dimensional NPS and the total 2-D NPS.

ACKNOWLEDGMENT

The authors would like to introduce great thanks to Dr. Saeed M. Al Kaabi the Chairman of Sharjah Education Council for his collaboration in the success of this work, and introducing support for all that is asked of him and also thanks to Mr. Mohamad Shameer the supervisor of the X-ray Center for Material Analysis at University of Sharjah in cooperation when using laboratory.

REFERENCES

[1] Z. A. Darwish, "Comparison of the noise power spectrumproperties of medical x-ray imaging systems," Universiti Teknologi Malaysia, Faculty of Science, 2011.
[2] D. L. Lee, L. K. Cheung, E. F. Palecki, and L. S. Jeromin, "Discussion on resolution and dynamic range of Se-TFT direct digital radiographic detector," in Medical Imaging 1996, 1996, pp. 511-522.
[3] J.-Y. Kim, J.-K. Park, J.-Y. Choi, B.-Y. Cha, S.-S. Kang, S.-H. An,S.-H. Nam, and H.-K. Choi, "Experimental evaluation of a-Se flat-panel X-ray detector for digital radiography," in Nuclear Science Symposium Conference Record, 2004 IEEE, 2004, pp. 4048-4052.
[4] J. T. Dobbins III, D. L. Ergun, L. Rutz, D. A. Hinshaw, H. Blume, and D. C. Clark, "DQE (f) of four generations of computed radiography acquisition devices," Medical Physics, vol. 22, pp. 1581-1593, 1995.
[5] J. T. Dobbins III, "Image quality metrics for digital systems," Handbook of medical imaging, vol. 1, pp. 161-222, 2000.
[6] J. T. Dobbins III, E. Samei, N. T. Ranger, and Y. Chen, "Intercomparison of methods for image quality characterization. II. Noise power spectruma)," Medical Physics, vol. 33, pp. 1466-1475, 2006.
[7] K. M. Hanson, "Simplified method of estimating noise-power spectra," in Medical Imaging'98, 1998, pp. 243-250.
[8] A. M. Bloomquist, J. Mainprize, G. Mawdsley, and M. Yaffe, "A task-based quality control metric for digital mammography," Physics in Medicine and Biology, vol. 59, p. 6621, 2014.
[9] K. Doi, "Scans in measuring Wiener spectra for photographic granularity," Japanese Journal of Applied Physics, vol. 5, p. 1213, 1966.
[10] R. F. Wagner, "Fast Fourier digital quantum mottle analysis with application to rare earth intensifying screen systems," Medical Physics, vol. 4, pp. 157-162, 1977.
[11] J. M. Sandrik and R. F. Wagner, "Radiographic screen-film noise power spectrum: variation with microdensitometer slit length," Applied optics, vol. 20, pp. 2795-2798, 1981.
[12] K. Doi, MTF's and Wiener Spectra of Radiographic Screen-film Systems, Volume II (including Speeds of Screens, Films and Screen-film Systems): US Department of Health and Human Services, Public Health Service, Food and Drug Administration, Center for Devices and Radiological Health, 1986.
[13]K. Koedooder, J. Strackee, and H. W. Venema, "A new method for microdensitometer slit length correction of radiographic noise power spectra," Medical Physics, vol. 13, pp. 469-473, 1986.
[14] A. Cowen and A. Workman, "A quantitative investigation of the noise processes in digital spot fluorography," Computers in Diagnostic Radiology eds. J. Robertson, P. Wankling, K. Faulkner and M. Holubinka (York: IPSM), 1990.
[15] W. M. S. W. Hassan, "Measurement of Wiener Spectrum of Radiographic Screen–Film Systems," Jurnal Teknologi, vol. 34, pp. 35–42, 2012.
[16] M. B. Williams, P. A. Mangiafico, and P. U. Simoni, "Noise power spectra of images from digital mammography detectors," Medical Physics, vol. 26, pp. 1279-1293, 1999.
[17]S. Suryanarayanan, A. Karellas, and S. Vedantham, "Physical characteristics of a full-field digital mammography system," Nuclear Instruments and Methods in Physics Research Section A: Accelerators, Spectrometers, Detectors and Associated Equipment, vol. 533, pp. 560-570, 2004.
[18]H.-S. Park, H.-J. Kim, H.-M. Cho, J. Jung, and C.-L. Lee, "Measurements and evaluation of the image noise power spectrum for computed radiography," in Nuclear Science Symposium Conference Record, 2008. NSS'08. IEEE, 2008, pp. 4378-4383.
[19]B. Lazzari, G. Belli, C. Gori, and M. R. Del Turco, "Physical characteristics of five clinical systems for digital mammography," Medical Physics, vol. 34, pp. 2730-2743, 2007.
[20] D. Zhang, H. Liu, and X. Wu, "DQE analysis on a dual detector phase x-ray imaging system," Physics in Medicine and Biology, vol. 53, p. 5165, 2008.
[21] W. M. S. W. Hassan and Z. A. Darwish, "Comparison of Two Methods of Noise Power Spectrum Determinations of Medical Radiography Systems," in Malaysia Annual Physics Conference 2010 (PERFIK2010), 2011, pp. 321-323.
[22] X. Liu and C. C. Shaw, "A-Si: H/CsI (Tl) flat-panel versus computed radiography for chest imaging applications: image quality metrics measurement," Medical Physics, vol. 31, pp. 98-110, 2004.
[23] E. Samei, "Image quality in two phosphor-based flat panel digital radiographic detectors," Medical Physics, vol. 30, pp. 1747-1757, 2003.
[24] H.-M. Cho, H.-J. Kim, C.-L. Lee, S. Nam, and J.-Y. Jung, "Imaging characteristics of the direct and mobile indirect digital radiographic systems," in Nuclear Science Symposium Conference Record, 2007. NSS'07. IEEE, 2007, pp. 3840-3846.

BIOGRAPHIES

Zeki Ahmed Darwish received a BSc degree in Physics in 1984 Basrah University, Iraq and MSc degree in Physics from UniversitiTeknologi Malaysia (UTM)in 2011under the supervision of Associate Professor Wan Muhamad Saridan Wan Hassan. He is currently a PhD candidate at Solar Energy Research Institute, National University of Malaysia (UKM). Lecturer of Physics at Ministry of Education in United Arab Emirates.

Wan Muhamad Saridan Wan Hassan received a BSc in Physics in 1982 from University Teknologi Malaysia (UTM), MScfrom University of California at Riverside USA in 1987 and PhD from Aberdeen University Scotland in 1998. He is currently an Associate Professor of Physics and Head of Physics Department, Faculty of Science, Universiti Teknologi Malaysia.

Amer Al-Nassiri received his Bachelor's degree in Electrical Engineering in 1977 from Basrah University, Iraq, the M.Sc. degree in Computer Engineering from Basrah University in 1979 and the Ph.D. degree in Computer Sciences from Basrah University in 1996. He had been working in Basrah University and in Jordan's Al-Isra University and Applied Sciences University. He is currently an Associate Professor at Ajman University of Sciences and Technology in UAE since 2002. His research interests include image and signal processing, Arabic character recognition, Steganography, computer and Internet Security and data compression.

.

Hussain Alawadhi received a BSc in Physics and Math from Iowa State University USA in 1988. He received his MSc and PhD from Purdue University USAin 1993 and 1999, respectively. He is currently an Associate Professor of Physics and Director of the X-ray Center for Material Analysis at the University of Sharjah, United Arab Emirates.